Effect of heat treatment on the microhardness of Ti-6Al-4V alloy fabricated by laser powder bed fusion and its prediction using machine learning

Jateen Shirodkar[1,2], *Shruti* Maheshwari[2*], *Vijaykumar* Jatti[3], and *Vikas* Gulia[2]

[1]Department of Mechanical and Automation Engineering, Shree Rayeshwar Institute of Engineering and Information Technology, Shiroda, Goa, 403103, India
[2]Department of Mechanical Engineering, Symbiosis Institute of Technology, Constituent of Symbiosis International (Deemed University), Mulshi, Pune, Maharashtra, 412 115, India
[3]Symbiosis Skill and Professional University, Pimpri-Chinchwad, Maharashtra, 412101, India

Abstract. Laser Powder Bed Fusion process of Additive manufacturing has evolved as a game-changing technology for creating highly sophisticated components for automotive, aerospace and medical applications. The impact as well as contribution of LPBF parameters, such as laser power as a source of energy, exposure time and hatch space in developing microhardness for Ti-6Al-4V alloy is explored using a Taguchi-based design of experiments. By employing an orthogonal array, the number of required experimental runs were reduced to nine by ensuring efficient parameter optimization. This study examines the post-processing effect of heat treatment on microhardness of Ti6Al4V alloy specimen, measured using Vickers hardness testing machine. Results obtained have demonstrated a notable hardness improvement after annealing which attributed to microstructural homogenization, reduced porosity and defect mitigation. Among the heat-treated samples, laser power emerged as the most influential parameter, with sample 4S (350 W laser power, 40 μs exposure time, 0.09 mm hatch spacing) achieving the highest microhardness of 543 HV, representing a 20.9% increase over as-built conditions. In the second phase, machine learning algorithms were implemented to develop predictive models of microhardness. The highest accuracy achieved by Random Forest with R^2=0.91 and Cat boost with R^2= 0.93 for as build and heat-treated samples respectively. Significant insights into process optimisation and property prediction of Ti-6Al-4V produced using LPBF are offered by this integrated experimental - computational approach.

1 Introduction

Customized products for industrial use and increased efficiency are now achievable owing to advancements in manufacturing technologies. Among these, Laser Powder Bed Fusion process is an efficient approach for producing metal, alloyed and composite components with

*Corresponding author : shruti.maheshwari@sitpune.edu.in

higher accuracy and capacity to fabricate intricate and personalized designs [1]. Laser Powder Bed Fusion is extensively explored to fabricate parts of titanium and titanium alloy with exceptional precision and mechanical performance, particularly in load-bearing implant and aerospace components [2]. With its high specific strength and resistance towards corrosion, Ti-6Al-4V alloy is consider to be a superior material used in aerospace and biomedical applications [3]. Furthermore, these elements have a major influence on the material's mechanical performance and microstructure evolution, controlling Laser Powder Bed Fusion (LPBF) effectively requires careful consideration of a wide range of interdependent printing parameters, including laser power, scan speed, layer thickness, hatch spacing, powder properties, along with thermal history [4]. Additive manufacturing is extremely sensitive towards processing parameters. Titanium and other alloys require precise parameter optimization for consistent performance. Important factors that control melt-pool dynamics, defect formation and thermal gradients which in turn control microstructure and mechanical properties usually include laser power (energy input), scan velocity (dwell time) and hatch spacing (track overlap). To improve mechanical reliability rigorous parametric studies and statistical optimization is must to achieve density and reduce heterogeneity [5]. Precise control on LPBF process demands structured approach to arrive at optimal condition by considering process variables like laser power, scan speed, hatch space, layer thickness, composition of powder, heat treatments etc. Combined effect of process parameters governs efficient melting, microstructural evolution and defect mitigation to develop mechanical and tribological characteristics of Ti-6Al-4V components. Robust experimental designs and statistical analyses are therefore essential to identify dominant factors, quantify parameter significance and establish repeatable, application-specific processing windows for reliable part qualification. [6,7]. However, further research is required to understand the intricate relation between various LPBF parameters, as these relationships are essential for developing mechanical response, microstructure stability and defect evolution.

A revolutionary method for creating intelligent, effective and incredibly dependable production systems is additive manufacturing. Complex, high-dimensional datasets produced during AM processes can be interpreted by integration of sophisticated Machine Learning (ML) frameworks [8]. These methods offer novel avenues for design validation, defect prediction and process parameter optimization. ML-driven models have shown great promise in the context of establishing a correlation between LPBF parameters, mechanical performance and microstructural characteristics, thus promoting predictive manufacturing techniques [9]. Thermal treatment is very essential in tailoring the mechanical and tribological properties by removing stresses which is responsible for creating a homogenised microstructure in LPBF made Ti-6Al-4V objects. Phase morphology, residual stress reduction and defect healing are all greatly impacted by post-processing procedures annealing, aging and cryogenic operations. These changes enhance Ti-6Al-4V's suitability for high end engineering applications by having a direct impact on its tensile strength, ductility, hardness and fatigue resistance. For additively manufactured parts to have a balance between strength and toughness, heat treatment conditions must be optimized [10,11]. Rapid thermal gradients and non-equilibrium solidification cause Ti-6Al-4V components produced by LPBF to frequently show high residual stresses and localized stress concentrations. The mechanical reliability in Ti-6Al-4V alloy part is increased by annealing treatments, which effectively reduce residual stresses, promote microstructural homogenization and improve dimensional stability [12]. The transition from the α’ to α along with development of β phase is possible by the annealing process [13].

In this research paper, few Machine Learning algorithms are used for predicting the microhardness of Ti-6Al-4V fabricated components. These algorithms are considered because of their ability to handle multi-dimensional datasets, capture nonlinear correlations and produce reliable predictions under a range of experimental circumstances. Application

of machine learning for LPBF studies is becoming more widely acknowledged as a potent instrument for maximizing process parameters, reducing experimental expenses and expediting material design. ML-based predictive frameworks allow the identification of dominant variables and their combined effects, where microstructure as well as mechanical response are extremely sensitive to changes in laser power, scan speed, hatch spacing and layer thickness. Compared with the traditional statistical methods, this approach enables more accurate material property forecasting.

To expand the data set available, data augmentation is used in the current study to create artificial datasets. This method overcomes a significant obstacle in the study of LPBF, where there is limited experimental data because of the high expense, time and resource requirements of lengthy trials. The reliability and generalizability of predictions for Ti-6Al-4V alloy components made by LPBF can be increased by growing the dataset in order to create more reliable Machine Learning (ML) models. In contrast to traditional statistical and empirical modelling techniques, machine learning offers a versatile framework that can capture the multi-factorial and nonlinear dependencies present in additive manufacturing processes. Machine learning algorithms have shown excellent conversion and accuracy in predicting mechanical and tribological properties by considering processing parameters like laser power, scan speed, hatch space etc as input values. Incorporating artificial intelligence using ML models, helps in identifying non-linear patterns, capturing hidden correlations and sensitive variables where traditional or conventional methods hinders to do so.

This research work helps in identifying the significance of processing parameters which are responsible for variation in microhardness of alloy produced through LPBF. Furthermore, the impact of post processing via annealing in enhancing the hardness is also explored. The best parameter combinations were identified using Taguchi design of experiments. Analysis of Variance is also utilized in further understanding the statistical relevance of the process parameters. In order to improve process understanding and facilitate data-driven optimization strategies, predictive models based on Machine Learning (ML) algorithms are created to forecast hardness in addition to these experimental methods. It is anticipated that this all-encompassing strategy will significantly advance LPBF, especially by lowering experimental expenses, minimizing trial-and-error and speeding up development cycles. Machine Learning algorithms like Random Forests, Cat Boost, Gradient Boosting, XG Boost and Linear Regression are used to predict microhardness based on input process parameters namely Laser Power, Exposure time and Hatch Space and later compared these values to those obtained from the experimentation. By taking into consideration the combined effects of several process variables, this method improves predictive accuracy by utilizing machine learning's ability to capture nonlinear and multidimensional relationships.

Materials section comprises of composition of Ti-6Al-4V powder and LPBF manufacturing process parameters indicating levels and factors. From an initial set of 27 possible runs, a reduced but representative experimental matrix is designed using a Taguchi L9 orthogonal array based on three parameters at three levels followed by heat treatment. The measured microhardness values are shown in the Results and Discussion section, along with interpretation of the impact of process parameters. Additionally, ML algorithms' ability to predict hardness is assessed. Lastly, the conclusion section highlights the uniqueness of this integrated approach, highlights the major contributions and offers suggestions for further research.

2 Materials

The CAD model was designed using SolidWorks software in accordance with relevant ASTM standards to find out microhardness, as illustrated in Figure 1. To produce specimens with high density, the Laser Powder Bed Fusion (LPBF) process is used by systematically

varying parameters namely laser power, scan speed, and hatch spacing, with a constant layer thickness of 0.06 mm.

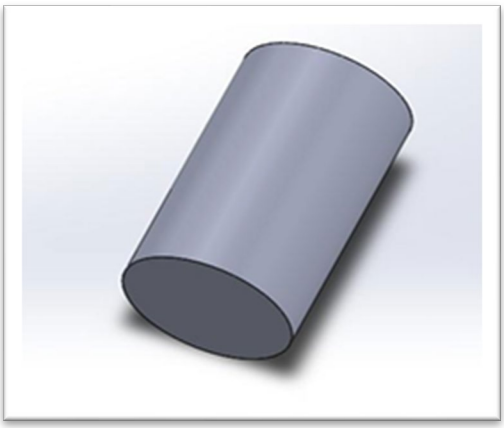

Fig. 1. A CAD model showing cylindrical specimen having 6 mm diameter and 10 mm length designed using SolidWorks.

Integration of Taguchi's orthogonal array with ANOVA has offered an efficient and statistically valid framework to explore and optimize LPBF parameters for Ti-6Al-4V alloy, with just nine targeted experimental runs. Ti-6Al-4V ELI powder having grain size of 30 μm was used that comprises up to 90% titanium by mass fraction alloyed using aluminium and vanadium up to 6.5% and 4.5% respectively.

The printing process parameters shown in below table 1. are determined with experts' opinion and existing literatures.

Table 1. Printing parameters for design of experiments.

Factors	**Laser Power**	**Exposure Time**	**Hatch Spacing**
Units	W	µs	mm
Level 1	300	40	0.08
Level 2	350	30	0.09
Level 3	375	20	0.1

Two sets of each combination were utilized to fabricate cylindrical specimens, having 6 mm diameter and height of 10 mm each. 3D printing was carried on Renishaw AM250 system, which operates based on the Laser Powder Bed Fusion technique to fabricate cylindrical bars directly from computer-aided design (CAD) models

3 Heat treatment

Objects produced by LPBF methodology uses extremely localised and rapid solidification which exhibits high residual stresses, non-equilibrium microstructures and anisotropy in the mechanical properties. Heat treatment unlocks the full potential of LPBF-printed Ti6Al4V parts by relieving stress, tuning microstructure, optimizing mechanical properties and making them suitable for high-end aerospace, biomedical and structural applications. The β-transus (Tβ) temperature for Ti6Al4V found to be 995 ± 5 °C using metallographic techniques. This research employed post-processing involving heat treatment under annealed conditions at

850 ± 10 °C for 2 hours to understand the impact of thermal treatment. Actual fabricated cylindrical bars are shown in Figure 2.

Fig. 2. Ti6Al4V alloy specimens fabricated using Laser Powder Bed Fusion Process. As build specimens are numbered from 1-9 while heat treated specimens are numbered from 1S-9S for identification and sample handling.

4 Microhardness

In the course of evaluating the microhardness of Ti-6Al-4V specimens fabricated through Laser Powder Bed Fusion (LPBF), Vickers microhardness testing was adopted due to its ability to measure hardness at the micro-scale with significantly smaller loads. It provided more consistent and meaningful data, especially for thin-walled features and regions near the melt pool or heat-affected zones. In light of this, microhardness measurements of the additively manufactured Ti-6Al-4V specimens were conducted at Praj Metallurgical Laboratory, Pune. A Vickers microhardness tester equipped with a diamond indenter of 136° pyramidal angle was employed for the analysis. The tests were performed using a consistent load of 0.1 kg applied for a dwell time sufficient to ensure stable indentation, as per standard microhardness testing protocols as shown in below mentioned Figure 3.

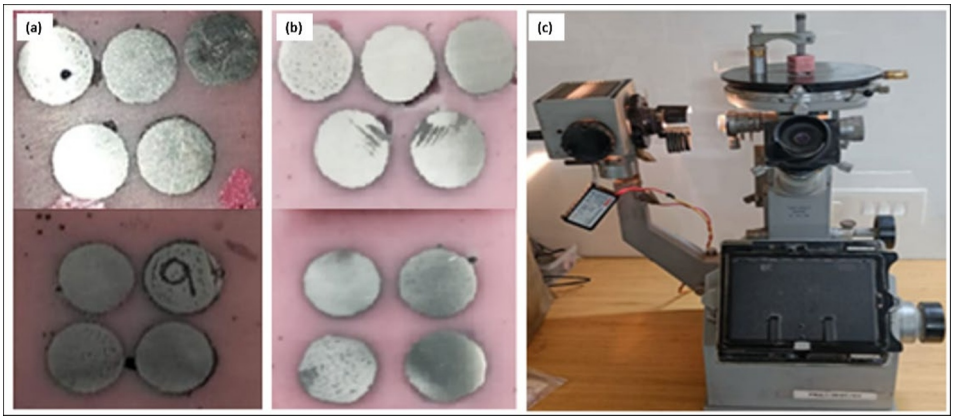

Fig. 3. Mounting of processed specimens and experimental setup employed for microhardness testing (a) As built Specimens, (b) Heat treated specimens, and (c) Vickers hardness tester employed.

A total of 18 samples were evaluated, comprising 9 as-built specimens and 9 that had undergone post-processing heat treatment. Each sample was carefully prepared through a standard metallographic polishing process to achieve a smooth surface finish suitable for accurate indentation. The indents were placed on polished cross-sections, ensuring uniform

spacing to avoid interference from neighbouring impressions. Microhardness values were recorded by using an optical microscope integrated with the hardness tester. Five indentations were recorded per sample for reliability and consistency in the recorded values of microhardness.

5 Machine learning

Microhardness of Ti-6Al-4V alloy fabricated using Laser Powder Bed Fusion (LPBF) process is predicted using regression-based machine learning (ML) algorithms. Statistical measures such as coefficient of determination (R^2), Root Mean Square Error (RMSE) and Mean Absolute Error (MAE) are used to systematically assess the predictive accuracy of these models. These metrics offer quantitative assessments of how well each model captures the relationship of process parameters with microhardness outcomes.

Limited data set for this research work is due to high costs and time-consuming characterization involved. To overcome this issue, artificial data set is generated using data augmentation process where in small number of actual experimental data points are converted into a larger set of synthetic data while maintaining the underlying statistical distribution and physical trends, as experimental data obtained through LPBF. ML algorithm's ability for generalization has improved and has also strengthen the training process resilience with this approach. The ML algorithms have captured non-linear trends between the process parameters like laser power, exposure time and hatch spacing in better way due to generation of the artificial data and mapping them with microhardness in both conditions.

During training and testing the dataset, each algorithm showed distinct advantages. Although it offered interpretability and insights into the direct linear contributions of process parameters, linear regression only served as a baseline model. However, when significant non-linearities were present, its predictive power was reduced. By dividing the dataset into parameter-specific decision rules, Random Forest increased prediction accuracy and were useful for capturing localized interactions. In order to get around this, Random Forests combined predictions from several trees as an ensemble technique, which improved accuracy, decreased variance and increased robustness in datasets.

The integration ML models and data augmentation provides a hybrid approach to optimize LPBF process parameters. These techniques are beneficial in multiple ways, as this approach makes it easier to generalise and predict microhardness with accuracy and also offers a way to cut down the expensive experimental trials. ML-driven approaches are a promising tool for improving predictive capabilities in additive manufacturing, as the comparative evaluation of models highlighted their significance of choosing appropriate algorithms based on dataset characteristics and complexity.

6 Results and discussion

6.1 Microhardness

The results obtained indicate that, in both conditions, processing parameters have a significant impact on developing microhardness of Ti-6Al-4V fabricated using LPBF. As-built samples microhardness values, which varied from 408 to 492 HV, demonstrated a significant reliance on the interaction of hatch spacing, exposure duration and laser power. Although excessive energy input resulted in localised coarsening and decreased hardness (Exp. 9 with 408 HV), higher laser power and optimised exposure improved microhardness. Hardness values increased under all conditions after heat treatment, ranging from 493 to 543 HV, demonstrating effective stress relief and microstructural homogenisation as a result of

α+β phase stabilisation. The increase in percentage was highly dependent on the parameters. The highest yields of 20.9% and 23.3% were obtained under moderate processing conditions, such as 350 W, 40 µs, 0.09 mm (Exp. 4) and 375 W, 20 µs, 0.09 mm (Exp. 9). This implies heat treatment relieved residual stresses and increased defect density, suboptimal as-built hardness benefited more from it.

Heat treatment continuously increased hardness by about 4–23%, demonstrating its significance in adjusting mechanical performance. The average value of microhardness for as build conditions and heat-treated conditions for each specimen and percentage increase after heat treatment are tabulated in table 2.

Table 2. Process parameters, average microhardness and percentage increase for each specimen.

Ex. No	Input Parameters				Microhardness (HV)		
	Laser Power (W)	Exposure Time (µs)	Hatch Spacing (mm)	Layer Thickness (mm)	As built	Heat treated	Percentage Increase (%)
1	300	40	0.08	0.06	477±1.73	499±1.73	4.612
2	300	30	0.09	0.06	464±2.31	493±1.73	6.250
3	300	20	0.1	0.06	438±1.44	478±1.44	9.132
4	350	40	0.09	0.06	449±2.02	543±1.73	20.935
5	350	30	0.1	0.06	492±1.15	513±1.73	4.268
6	350	20	0.08	0.06	478±4.62	515±1.44	7.740
7	375	40	0.1	0.06	485±2.89	504±2.31	3.917
8	375	30	0.08	0.06	457±1.73	535±2.89	17.067
9	375	20	0.09	0.06	408±1.73	503±1.44	23.284

The bar graph shown in Figure 4 compares microhardness values for as-built with Heat heat-treated samples of Ti6Al4V alloy fabricated by LPBF. Each experiment shows microhardness enhancement after undergoing heat treatment.

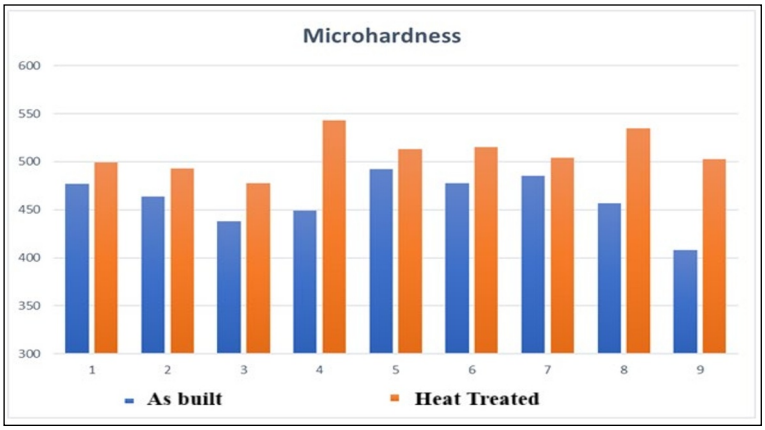

Fig. 4. Bar chart showing Vickers mirohardness values for as built and heat treated samples.

Standard Deviation was computed based on multiple indentations made in various areas of every specimen in order to evaluate reliability of the Vickers microhardness

measurements. In all cases, the measured hardness values showed small standard deviations, with minimal local variation having good consistency. Some samples, like Experiment 6, displayed greater deviation (Approx. 4.62), due to porosity across the cross section which was noted in as built specimen. The statistical representation and dependability of the reported result is enhanced by incorporating standard deviation in the hardness data.

6.2 Taguchi method and ANOVA-based optimization for microhardness of LPBF fabricated Ti6Al4V for as built conditions

The main effect plots of signal-to-noise (S/N) ratio against individual process parameters (laser power, exposure time and hatch spacing) provide insight into their relative influence on microhardness in the as-fabricated specimens. Main effect plots for microhardness of as built specimen are shown in Figure 5.

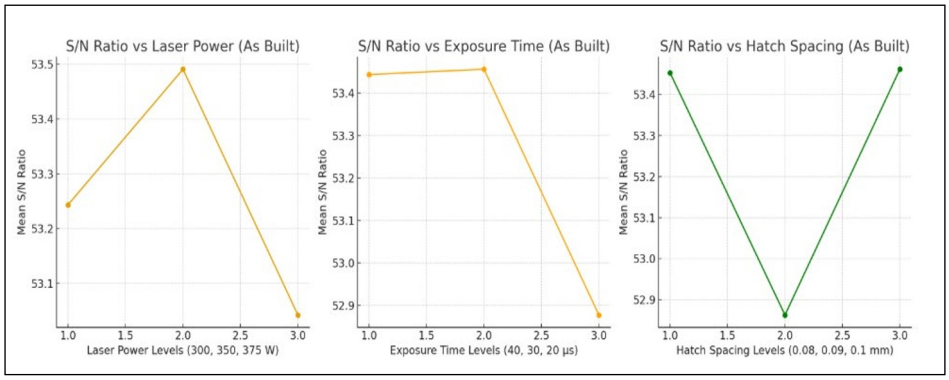

Fig. 5. Main effect plots signal to noise ratio for laser power, exposure time and hatch spacing levels for microhardness of as built specimens.

The S/N ratio for Laser Power has increased gradually from Level 1 (300 W) to Level 2 (350 W), At Level 3, it started decreasing (375 W). According to this, 350 W is the ideal temperature, indicating that excessive power causes over-melting and porosity, moderate energy input guarantees stable melting and minimizes the formation of defects. When the exposure time was lowered from 40 µs to 20 µs, the S/N ratio steadily dropped. This pattern suggests that extended exposure enhances melt pool stability and facilitates better powder particle consolidation. Very brief exposure periods, however, restrict energy absorption and raise the possibility of defect generation. As hatch spacing increased, the S/N ratio dropped; the lowest value (0.08 mm) showed the best performance. Higher overlap between neighbouring laser tracks is encouraged by narrower spacing, which lowers porosity and improves densification. On the other hand, greater hatch spacing causes inadequate track bonding, which deteriorates mechanical qualities.

Overall, 350 W laser power, 40 µs exposure time and 0.08 mm hatch spacing were determined to be the ideal parameters for optimizing microhardness in the as-fabricated condition. The three factors that had the biggest effects were exposure time, hatch spacing and laser power as shown in table 3 while ANOVA results and effect control factors for as built condition are tabled in table 4.

Table 3. Signal to Noise table and effect ranking for as built conditions.

Factor	Level 1	Level 2	Level 3	Delta	Rank
Laser Power (W)	53.243	53.491	53.042	0.449	3
Exposure Time (μs)	53.443	53.456	52.877	0.579	2
Hatch Spacing (mm)	53.452	52.863	53.461	0.598	1

Table 4. ANOVA results and effect control factors for as built.

Source	DF	Seq SS	Adj SS	Adj MS	F	P
Laser Power (LP)	2	2685.8	2685.8	1342.9	5.65	0.151
Exposure Time (ET)	2	3069.6	3069.6	1534.8	6.45	0.134
Hatch Spacing (HS)	2	3150.5	3150.5	1575.3	6.62	0.131
Residual Error	2	476.0	476.0	238.0	–	–
Total	8	9381.9	–	–	–	–

6.3 Taguchi method and ANOVA-based optimization for microhardness of LPBF fabricated Ti6Al4V for heat treated conditions

For Heat treated samples, the main effect plots of signal-to-noise (S/N) ratio against laser power, exposure time and hatch spacing after heat treatment (850 °C/ 2hr, furnace cooled) highlight the influence of process parameters on the improved microhardness of the specimens. Main effect plots for microhardness of heat-treated specimen are shown in Figure 6.

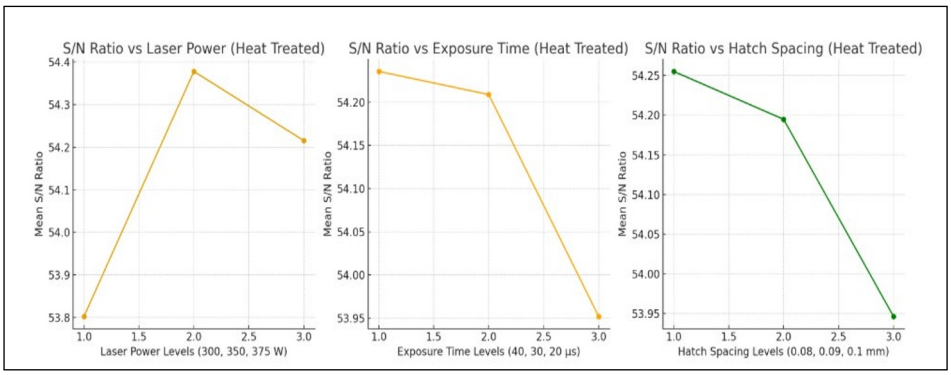

Fig. 6. Main effect plots signal to noise ratio for laser power, exposure time and hatch spacing levels for microhardness of heat treated specimens.

S/N ratio for laser power has increased gradually from Level 1 (300 W) to Level 3 (375 W), in contrast to the as-fabricated conditions as heat treatment refined the microstructure created under high-energy input and reduced residual stresses, this trend indicates that higher laser power resulted in a more homogenous microstructure after annealing. S/N ratio for exposure time exhibited a declining trend. The long exposure time (40 μs) resulted in improved melting and densification, which heat treatment further stabilized. The highest S/N ratio was obtained with the smallest hatch spacing (0.08 mm), whereas performance was lowered by wider spacing because of insufficient bonding. However, by encouraging defect healing, heat treatment mitigated the adverse effects of greater spacing to some extent.

Overall, 375 W laser power, 40 μs exposure time, and 0.08 mm hatch spacing were found to be the ideal parameters for optimizing microhardness following heat treatment. After annealing, laser power became the most important factors compared to the as-fabricated state as shown in table 5. This comparison shows that heat treatment changed the relative

importance of process parameters, especially enhancing the beneficial role of laser power, while also improving microhardness under all conditions. ANOVA results are also shown in table no 6.

Table 5. Signal to noise table and effect ranking for heat treated specimen.

Factor	Level 1	Level 2	Level 3	Delta	Rank
Laser Power (W)	53.803	54.378	54.216	0.576	1
Exposure Time (µs)	54.236	54.209	53.952	0.284	3
Hatch Spacing (mm)	54.255	54.195	53.947	0.309	2

Table 6. ANOVA results and effect control factors for heat-treated specimens.

Source	DF	SS	Adj SS	Adj MS	F	P
Laser Power (LP)	2	4590.7	4590.7	2295.4	11.9	0.078
Exposure Time (ET)	2	2265.3	2265.3	1132.6	5.87	0.146
Hatch Spacing (HS)	2	2495.6	2495.6	1247.8	6.47	0.134
Residual Error	2	386.2	386.2	193.1	–	–
Total	8	9737.8	–	–	–	–

Tables number 4 and 6 containing ANOVA results of as built and heat-treated samples shows the P-values for laser power, exposure time and hatch spacing greater than 0.05. Hence, at the 95 % confidence level, their effects on microhardness are indicative. However, the relatively high F-values suggest a meaningful impact of parameters. The absence of statistical significance is majorly due to limited number of experimental data set and the corresponding low degrees of freedom for the residual error, which reduce the ANOVAs statistical power. These findings provide basis for process optimization, while future studies with more replicas are recommended to confirm statistical significance.

6.4 Energy dispersive X-ray analysis (EDS)

The EDS research sheds important light on the connection between Ti-6Al-4V's microhardness and chemical composition in both as-built and heat-treated forms. Elemental distribution for experiment number 4 where maximum hardness was achieved with an 21% increase in microhardness after heat treatment is tabulated in table 7 and EDS spectra is shown in Figure 7.

Table 7. Elements distribution of Ti6Al4V for sample 4 (As Build) and 4S (Heat Treated).

Expt No	Ti	Al	V	C	O	Na	N	Fe
	Wt %	Wt %	Wt %	Wt %	Wt %	Wt %	Wt %	Wt %
4	71.2	4.9	3.4	7.2	13.3	-	-	-
4S	70.0	3.8	3.3	4.1	15.2	1.7	1.5	0.5

Titanium accounted for 71.2 weight percent of the as-built Ti-6Al-4V according to EDX analysis, followed by aluminium (4.9 weight percent), vanadium (3.4 weight percent), oxygen (13.3 weight percent) and carbon (7.2 weight percent). Due to partial oxidation and hydrocarbon contamination, LPBF often has elevated oxygen and carbon concentrations, which strengthens solid-solution but may also provide embrittlement problems. Titanium remained predominant (70.0 wt.%) with heat treatment, but aluminium and vanadium somewhat declined. As a result of diffusion and environmental interactions during thermal exposure, the oxygen content increased to 15.2 weight percent, the carbon content decreased to 4.1 weight percent and new elements such nitrogen (1.5 weight percent), sodium (1.7

weight percent), and iron (0.5 weight percent) emerged. In comparison to the as-built state, the microhardness rose by about 21% to 543 HV.

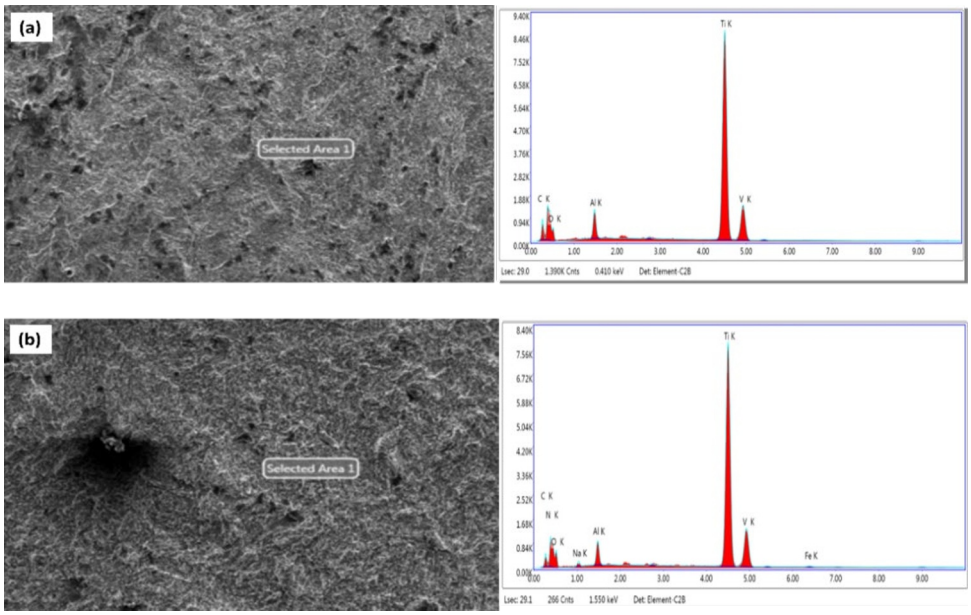

Fig 7. EDS Spectra of sample 4 (350 W laser power, 40 µs exposure time, 0.09 mm hatch spacing). (a) Sample 4 (As Built), and (b) Sample 4S (Heat treated).

EDS data for heat treated sample when compared to as built, the increase in Oxygen (O) content and the introduction of Nitrogen (N), is identified which is critical for change in hardness values. Oxygen and nitrogen are potent alpha-stabilizers in titanium and are known to dissolve interstitially within the hexagonal close-packed (α-Ti) crystal structure. Interstitial solid-solution strengthening is a highly effective mechanism. The small traces of oxygen and nitrogen atoms can occupy the voids in the titanium lattice. Since these atoms are larger than the available space, they introduce significant localized strain fields and lattice distortion. Distorted regions act as strong obstacles to the movement of dislocations (the crystallographic defects for plastic deformation). By impeding dislocation motion, the material requires a much higher stress to deform plastically, which is macroscopically observed as a significant increase in hardness. Therefore, the EDS results directly support the conclusion that the improved hardness is due to the solid-solution strengthening provided by the heat-induced incorporation of these interstitial light elements.

This improvement is associated with interstitial strengthening by oxygen and nitrogen. The findings show that heat treatment considerably increases hardness in addition to stabilizing and redistributing interstitials. To improve mechanical performance, LPBF-produced Ti-6Al-4V can be tailored through rigorous post-processing that balances compositional effects and microstructural refinement.

6.5 Machine Learning

Data augmentation was used to improve model resilience and overcome the drawbacks of short experimental datasets. Nine experimental data points derived from methodically varying process parameters made up the original dataset. A total of 59 data points were produced for each condition (as-built and heat-treated) after an additional 50 artificial data

points were created by augmentation. The augmentation methodology ensured that generated data points remained realistic in nature while increasing the design space by using synthetic interpolation and perturbation of existing process parameters within physically acceptable limits. This method maintained metallurgical significance while avoiding extrapolation outside of the process window. By verifying statistical coherence with the original dataset and examining the physical feasibility of hardness predictions, the additional data were validated. Since machine learning algorithms typically need larger datasets to capture complicated, nonlinear connections, our approach greatly enhanced model training. The model's ability to generalize was improved by augmentation, which decreased the possibility of overfitting to the small number of initial points. Its capacity to offer a more thorough mapping of process–property correlations without requiring extensive experimental trials which are expensive and time-consuming in additive manufacturing, making this enhancement significant. By expanding data points, it is easier to identify patterns in process parameter before and after heat treatment conditions, making comparisons between algorithms more equitable and simultaneously increases the accuracy of predictive modelling.

In order to capture the trends and predict the microhardness (HV) of Ti-6Al-4V alloy fabricated via LPBF under both as-built and heat-treated circumstances, several machine learning regression models were employed and examined. To arrive at the conclusion in determining which algorithm has captured the trend in most significant manner, standard statistical measures such as R^2 (coefficient of determination), RMSE (root mean square error), MSE (Mean Squared error) and MAE (mean absolute error) were assessed for each approach. Excellent prediction accuracy was demonstrated by Random Forest, which consistently obtained the greatest R^2 value of 0.91 in as built condition. Linear regression performed worse than ensemble approaches due to its inability to capture nonlinear interactions among the various process factors.

Overall, ensemble methods (Random Forest, cat boost, Gradient Boosting and XG Boost) demonstrated the best agreement with experimental hardness values, effectively reducing prediction errors and capturing the nonlinear effects of laser power, exposure time and hatch spacing. Actual verses Predicated values for as built by ML algorithms are presented by visual findings in Figure 8, whereas comparison of actual and predicted microhardness values of heat-treated specimens by ML algorithms are displayed in Figure 9.

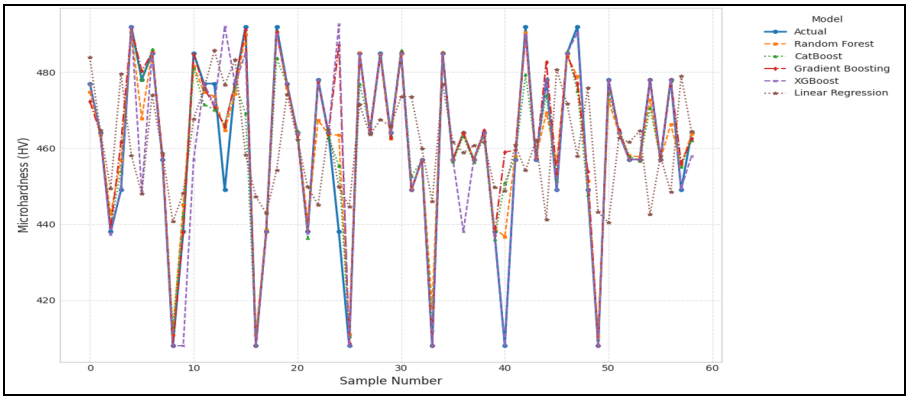

Fig. 8. Comparison of actual and predicted values of microhardness for as built specimens by machine learning models.

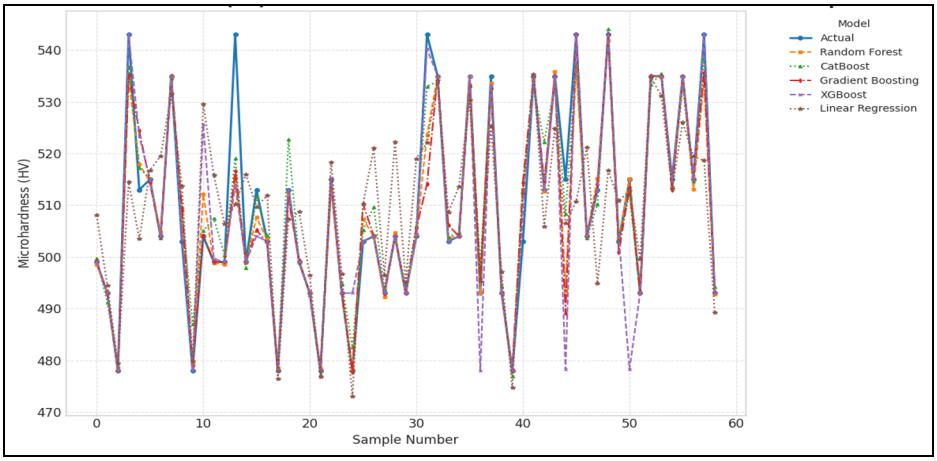

Fig. 9. Comparison of actual and predicted values of microhardness for heat treated specimens by machine learning models.

The impact on actual datasets was substantial, and predictions closely aligned with experimental values, indicating that these models can be reliably extended to unseen parameter ranges for process optimization. ML algorithms were also used to train the data set of the heat-treated samples. The finding showed slightly improved performance as compared to heat treated samples with Cat Boost yielding R^2 = 0.93. The performance matrices are mentioned in table 8.

Table 8. Performance parameters for as built and heat-treated specimen.

As Built Samples					**Heat Treated Samples**				
Model	R^2	RMSE	MAE	MSE	Model	R^2	RMSE	MAE	MSE
Random Forest	0.91	6.90	3.85	47.68	Cat Boost	0.93	4.94	3.01	24.48
Cat Boost	0.88	8.14	4.05	66.27	Random Forest	0.90	5.96	2.60	35.54
Gradient Boosting	0.82	9.98	3.40	99.74	Gradient Boosting	0.87	6.86	2.81	47.11
XG Boost	0.75	11.78	4.05	138.86	XG Boost	0.78	8.90	3.162	79.36
Linear Regression	0.12	22.06	16.98	486.71	Linear Regression	0.58	12.43	9.25	154.74

Although the relative importance of process parameters changed, the model accuracy for the heat-treated dataset stayed good. Although ensemble algorithms were still able to produce R^2 values above 0.75, somewhat larger RMSE values were noted, most likely as a result of heat treatment-induced microstructural homogeneity. This implies that although trends could still be captured by the models, predictions were less susceptible to small changes in parameters because of decreased hardness variability following heat treatment. RMSE and MAE were essential in measuring absolute prediction errors in hardness values, which are directly pertinent for engineering applications, while R^2 alone is insufficient to evaluate model performance overall. Strong predictive fidelity was proven by the combination of high R^2 and low RMSE, particularly for Random Forest and Cat Boosting in as built and heat-

treated samples respectively, highlighting their applicability for modelling intricate additive manufacturing datasets. These observations emphasize how important it is to consider statistical markers in estimating the robustness of the model under various material conditions. Correlation heatmap for as built and Heat-treated samples are plotted for better understanding and mentioned in Figure 10.

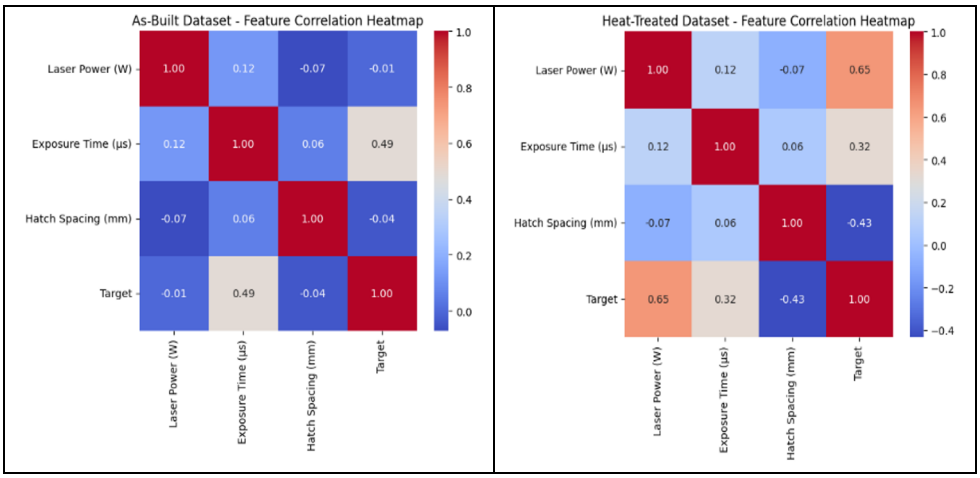

Fig. 10. Correlation heatmap for as built samples and Heat-treated sample.

7 Conclusion

Vickers microhardness scale is more reliable for accurate micro-mechanical characterization of additively manufactured titanium alloy components due to its precision, small load handling capability and adaptability to fine AM microstructures. Effect of heat treatment on microhardness enhancement of Ti6Al4V alloy using LPBF were thoroughly examined in this work. It was observed that laser power has strong impact on the heat-treated Ti6Al4V alloy's microhardness. Specimen printed with a 350 W laser power, 40 µs exposure duration and 0.09 hatch distance followed by heat treatment, showed maximum hardness value of 543 HV. Post processing heat treatment has significantly improved the microhardness of LPBF-fabricated Ti6Al4V samples (up to 23% increase), particularly for high-energy input conditions. Combination of higher laser power, short exposure time and moderate hatch space has resulted in microstructure that has significantly benefited from heat treatment by achieving the highest hardness improvement percentage. This makes it the most suitable setting for applications requiring high-strength Ti6Al4V components with efficient post-processing potential.

Laser power emerged as the dominant factor, as annealing minimized residual stresses and stabilises the microstructures formed under higher energy input. Random Forest algorithm had the highest accuracy among the ML algorithms evaluated for microhardness prediction under build conditions, with an R^2 value of 0.91, an RMSE of 6.90, an MAE of 3.85 and an MSE of 47.68. In contrast, Cat Boost displayed an R^2 value of 0.93, an RMSE of 4.94, an MAE of 3.01, and an MSE of 24.48 for heat treated samples. Linear regression has failed to capture the nonlinear trends in the data set and significantly underperformed. Future research should examine in-depth how various scan techniques, layer thickness, construction orientations and other heat treatment methods affect microhardness. Other microhardness test like knoop may be explored.

References

1. M. Arunadevi and V. N. V. Bhandarkar, “Surface Roughness Prediction Using ANN Regression and Classification Model for S30C Alloy Metals Parts Manufactured by Laser Powder Bed Fusion,” J. Inst. Eng. Ser. D, (2024). https://doi.org/10.1007/s40033-024-00840-3
2. H. Y. Ma et al., “Advances in additively manufactured titanium alloys by powder bed fusion and directed energy deposition: Microstructure, defects, and mechanical behavior,” J. Mater. Sci. Technol., **vol. 183**, pp. 32–62 (2024). https://doi.org/10.1016/j.jmst.2023.11.003
3. S. McConnell, Y. Beshay, K. Kourousis, and D. Tanner, “Increasing productivity for laser powder bed fusion of Ti–6Al–4V parts through increased layer thickness,” Prog. Addit. Manuf., no. 0123456789 (2025). https://doi.org/10.1007/s40964-025-01079-4
4. M. Gor et al., “A critical review on effect of process parameters on mechanical and microstructural properties of powder-bed fusion additive manufacturing of ss316l,” Materials (Basel)., **vol. 14**, no. 21 (2021). https://doi.org/10.3390/ma14216527
5. A. Paraschiv, G. Matache, M. R. Condruz, T. F. Frigioescu, and L. Pambaguian, “Laser Powder Bed Fusion Process Parameters’ Optimization for Fabrication of Dense IN 625,” Materials (Basel)., **vol. 15**, no. 16 (2022). https://doi.org/10.3390/ma15165777
6. B. Gaur, R. Ghyar, and R. Bhallamudi, “Parameter Optimization for Printing Ti6Al4V-Alloy Patient-Customized Orthopaedic Implants by Laser Powder Bed Fusion Using Physio-mechanical Properties and Biological Evaluations,” Indian J. Orthop., **vol. 56**, no. 5, pp. 797–804 (2022). https://doi.org/10.1007/s43465-021-00577-1
7. M. B. and E. A. Behzad Fotovvati, Modeling and Optimization Approaches of Laser-Based Powder-Bed Fusion Process for Ti-6Al-4V Alloy" Coatings **2020**, pp. 1–29, (2020). https://doi.org/10.3390/coatings10111104
8. S. Xiao, J. Li, Z. Wang, Y. Chen, and S. Tofighi, “Advancing Additive Manufacturing Through Machine Learning Techniques: A State-of-the-Art Review,” Futur. Internet, **vol. 16**, no. 11 (2024).https://doi.org/10.3390/fi16110419
9. S. Kumar et al., “Machine learning techniques in additive manufacturing: a state of the art review on design, processes and production control,” J. Intell. Manuf., **vol. 34,** no. 1, pp. 21–55, (2023). https://doi.org/10.1007/s10845-022-02029-5
10. J. Sarma, R. Kumar, A. K. Sahoo, and A. Panda, “Enhancement of material properties of titanium alloys through heat treatment process: A brief review,” Mater. Today Proc., **vol. 23**, no. xxxx, pp. 561–564, (2020). https://doi.org/10.1016/j.matpr.2019.05.409
11. P. O. Omoniyi, E. T. Akinlabi, and R. M. Mahamood, “Heat Treatments of Ti6Al4V Alloys for Industrial Applications: An Overview,” IOP Conf. Ser. Mater. Sci. Eng., **vol. 1107,** no. 1, p. 012094, (2021).https://doi.org/10.1088/1757-899X/1107/1/012094
12. Z. Xiao et al., “Residual stress, microstructure and micro-hardness evolution of laser powder bed fusion Ti6Al4V: Effect of stress relief annealing,” J. Mater. Res. Technol., **vol. 37,** no. May, pp. 3815–3821, (2025). https://doi.org/10.1016/j.jmrt.2025.07.039
13. Y. Xu, Y. Lu, K. L. Sundberg, J. Liang, and R. D. Sisson, “Effect of Annealing Treatments on the Microstructure, Mechanical Properties and Corrosion Behavior of Direct Metal Laser Sintered Ti-6Al-4V,” J. Mater. Eng. Perform., **vol. 26**, no. 6, pp. 2572–2582, (2017). 10.1007/s11665-017-2710-y